A poromechanics approach to assess the effect of frost heave on double-barrel culverts in cold regions

Hongwei Liu, Pooneh Maghoul, & Ahmed Shalaby
University of Manitoba, Winnipeg, Manitoba, Canada
Amir Khatibi
Transportation Division (Infrastructure), Government of the Northwest Territories, Canada

ABSTRACT
The serviceability of infrastructure such as buried utilities, pavement structures, and building foundations in cold regions can be adversely affected by seasonal frost actions in cold regions. Frost actions on road structures including culverts can be more complicated to assess and mitigate due to the existing double-cooling sources, i.e. pavement surface and subsurface culverts openings. Culverts are used as a waterway under a road and their structural integrity has an impact on the road roughness. Multi-physics analysis including heat transfer, mass transfer and mechanical analysis is required to explain thoroughly the formation of ice lenses in frost-susceptible soils. This paper aims to numerically study the distribution of temperature and pore-water pressure during the freezing process as well as the deformation in the soil due to frost heave by using a coupled Thermo-Hydro-Mechanical (THM) model in the framework of the mechanics of porous media.

RÉSUMÉ
Le fonctionnement des infrastructures telles que les infrastructures enterrées, les structures de chaussée, et les fondations des bâtiments dans les régions froides peut être affecté négativement par les actions du gel. Toutefois, ces actions sur les structures de route incluant les ponceaux peuvent être plus compliquées à évaluer et à atténuer en raison des doubles sources de refroidissement existantes, c'est-à-dire des ouvertures de ponceaux souterrains et la surface de la chaussée. Les ponceaux sont utilisés comme une voie navigable sous une route et leur intégrité structurelle a un impact sur la rugosité de la route. Une analyse multi-physique comprenant le transfert de chaleur, le transfert de masse et l'analyse mécanique est nécessaire pour expliquer de manière approfondie la formation de lentilles de gel dans les sols sensibles au gel. Cet article vise à étudier numériquement la distribution de la température et de la pression interstitielle au cours du processus de gel ainsi que la déformation du sol due au soulèvement au gel en utilisant un modèle couplé Thermo-Hydro-Mécanique (THM) dans le cadre de la mécanique des milieux poreux.

1 INTRODUCTION

Frost action in soils can cause detrimental damage to buried utilities, pavement and other infrastructures. Three essential factors for detrimental frost action are (a) subfreezing temperature, (b) continual supply of water (a high water table), and (c) presence of frost-susceptible soils. If one of these conditions is not met, frost action will not occur. For example, in a pavement structure, if the temperature at the level of the frost-susceptible subgrade is above the freezing point, frost heave will be preventable. Furthermore, it is worth noting that a good infiltration drainage system in the pavement structure, per se, cannot prevent frost heave as long as there are subfreezing temperature and a high-water table that provides the frost-susceptible subgrade with continual upward water supply.

Ice lenses are formed when enough water migrates to the freezing front and it causes excessive deformations in frost-susceptible soils (Liu et al. 2019). The formation of ice lenses is also very sensitive to both the duration and intensity of the freezing temperature. A fast propagation of freezing front due to the quick drop of temperature will not lead to the formation of ice lenses and all water will freeze in the pores (in-place freezing); a slow rate of cooling, however, provides sufficient time for water to migrate and ice lenses are likely to grow. Both the heaving and thawing phases of frost action often lead to cracking in the pavement surface, which results in reduction in the life of a pavement and annual costs due to rehabilitation programs. The damage cost due to the adverse effects of frost heave on infrastructure is estimated to be up to billions of dollars every year.

This paper presents a coupled Thermo-Hydro-Mechanical (THM) model in the framework of the theory of poroelasticity using a porosity rate function. The aim is to numerically study the distribution of temperature and pore-water pressure during the freezing process as well as the deformation in the soil due to frost heave. It takes into consideration the effect of both frost heave and soil consolidation by adapting the effective stress analysis approach for the transient problems. This can be considered as a considerable advantage for modeling frost heave and studying the effect of overburden pressure on frost-susceptible soils. The model is fully verified by comparing the numerical results with different laboratory test data found in the literature. Afterwards, the model is applied to study the distribution of temperature and pore-water pressure in the ground as well as the amount of frost heave and differential deformations at the pavement surface in Manitoba, Canada. The culvert sites have been

instrumented with thermistors as part of the monitoring program of the ground thermal profile near the culvert openings since 2016 (Moussa et al. 2018). The frost heave phenomenon for culvert structures is comprehensively investigated by studying the effect of overburden pressure and temperature variation. The real weather data is used for the numerical modelling. Also, to mitigate frost heave and differential displacements at the road surface, different insulation methods are considered to evaluate the effect of the position of insulation near the culverts on frost heave at the pavement surface. The outcomes of this research can be used for the design or rehabilitation program of culvert structures in cold regions.

2 MODEL DESCRIPTION

2.1 Kinematic Assumptions

The linearized form of Green-Lagrange strain tensor, ε_{ij} for infinitesimal deforamtion is

$$\varepsilon_{ij} = \frac{1}{2}(u_{i,j} + u_{j,i}) \quad [1]$$

The skeleton's volume dilatation ε_{ij} is required to match the variations of connected pore spaces (or porosity) n because of the incompressibility of solid grains. Assumed constitutive rules are described next.

2.2 Constitutive Model

The constitutive law of the solid skeleton describing the stress-strain relations, in a rate form, is defined in terms of the effective stress $\sigma'_{ij} = \sigma_{ij} - \alpha p\delta_{ij}$, as

$$d\sigma'_{ij} = D_{ijkl}\, d\varepsilon^m_{kl} \quad [2]$$

where σ_{ij}, α, p. D_{ijkl} and ε^m_{kl} are the total stress, the Biot coefficient, the pore-water pressure, the fourth order stiffness tensor and the strain tensor due to the effective stress change in a freezing soil, respectively.

The total strain increment consists of two components due to: (i) the expel of the porewater or the effective stress change $d\varepsilon^m_{ij}$, and (ii) the porosity growth because of the formation of ice lenses, $d\varepsilon^{ice}_{ij}$. Subsequently

$$d\varepsilon^m_{ij} = \mathrm{d}\varepsilon_{ij} - d\varepsilon^{ice}_{ij} \quad [3]$$

where $d\varepsilon^{ice}_{ij}$is defined in terms of porosity rate and porosity growth tensor.

The stress-strain constitutive equation given in Equation (2) can be rewritten as

$$d\varepsilon^m_{ij} = \frac{1+\mu}{E} d\sigma'_{ij} - \frac{\mu}{E} d\sigma'_{kk}\delta_{ij} \quad [4]$$

where in which *E* and μ are the Young's modulus and Poisson's ratio, respectively. This equation in terms of total stress and pore water pressure becomes:

$$d\varepsilon^m_{ij} = \frac{1}{2G}\left(d\sigma_{ij} - \frac{\mu}{1+\mu} d\sigma_{kk}\delta_{ij}\right) + \frac{\alpha}{3K} dp\delta_{ij} + d\varepsilon^{ice}_{ij} \quad [5]$$

where *G* and *K* are the shear and bulk modulus, respectively.

The dependency of the mechanical parameters to the latent heat (porewater phase change) is considered in the Young's modulus by defining the frozen and unfrozen Young's module. A step function is then defined to make the transition possible in the model.

For the fluid phase, on the other hand, the adopted constitutive model in the water flux within the soil skeleton, q^w_i, is the one's of Darcy-Buckingham as

$$q^w_i = -K^H_{ij}\left(\frac{p_{,i}}{\gamma_w} + g_j \mathrm{z}\right) \quad [6]$$

where $K^H_{ij}$and z are the hydraulic conductivity tensor and an elevation head, respectively. Hence $-K^H_{ij} = -K^H\delta_{ij}$ in an isotropic situation. The hydraulic conductivity $-K^H$ is temperature dependent. As temperature decreases, the unfrozen water content reduces. The corresponding hydraulic conductivity (mainly depends on the value of unfrozen water content), also decreases.

The well-known Furrier's law is chosen as the constitutive equation relating temperature, T, and heat flux, q^T_i. Thus

$$q^T_i = -\lambda_T T_{,i} \quad [7]$$

in which λ_T is the total thermal conductivity of the soil defined as

$$\lambda_T = \theta_w\lambda_w + \theta_i\lambda_i + \theta_s\lambda_s \quad [8]$$

where λ_w , λ_i , and λ_s are the thermal conductivities of water, ice, and solid skeleton, respectively.

The porosity rate function was introduced originally by (Michalowski 1993) to determine the soil volume increase due to the ice growth. This describes an increase in the soil porosity that is induced by the migration of porewater into the freezing fringe where the pore-water freezes. The porosity rate function allows to consider the effect of the formation of ice lenses on the solid skeleton deformation without introducing the ice pressure in the constitutive rule. The porosity rate $\dot{\theta}$ due to in-situ freezing and ice lens formation is defined:

$$\dot{\theta} = \dot{\theta}_m \left(\frac{T-T_0}{T_m}\right)^2 e^{1-\left(\frac{T-T_0}{T_m}\right)^2} \frac{\left\|\frac{\partial T}{\partial l}\right\|}{g_T} e^{-\|\sigma_{kk}\|/\zeta} \quad [9]$$

where $\dot{\theta}_m$ is the maximum porosity rate. Furthermore, T_m, T_0, T, $\left\|\frac{\partial T}{\partial l}\right\|$and σ_{kk} denote temperature occurring at the maximum porosity rate, freezing point of water, the soil's temperature, the temperature gradient and first invariant of the total stress, respectively. σ_{kk} can be calculated as σ_{11}+ σ_{22}+ σ_{33} . g_T and ζ are two constant parameters. The porosity growth tensor is defined to specify the growth direction of ice lenses, such that

$$\dot{\theta}_{ij} = \dot{\theta}\,\alpha_{ij} \quad [10]$$

where

$$\alpha_{ij} = \begin{bmatrix} \xi & 0 & 0 \\ 0 & (1-\xi)/2 & 0 \\ 0 & 0 & (1-\xi)/2 \end{bmatrix}$$

The value of ξ ranges from 0.33 to 1. An isotopic and one-dimensional ice lenses growth corresponds to ξ = 0.33 and ξ = 1, respectively. By setting ξ as one, the frost heave is assumed to develop at the temperature gradient direction. The strain tensor due to the frost effect, $d\varepsilon_{ij}^{ice}$, is

$$d\varepsilon_{ij}^{ice} = \dot{\theta}_{ij} dt \quad [11]$$

The parameters used in the porosity rate function are determined from the calibration process using freezing tests (Michalowski et al. 2006). The freezing lab tests can have various overburden pressure, initial soil temperature (or temperature gradient). Based on the data from lab test, we can determine the porosity rate function parameters that best fit lab results using least square techniques. However, it is found that the most important parameter that differentiates soil types is the maximum porosity rate value $\dot{\theta}_m$. This value has been recommended by (Michalowski et al. 2006) to be 4 (1/day) and 17 (1/day) for clay and silt, respectively. Normally, this value for other soil types can be roughly taken between 4 and 17 (1/day). However, a lower value can also be used to make soil less frost susceptible, which is mainly due to the lack of comprehensive lab data (Zhang et al. 2015).

2.3 Conservation Laws

The conservation of linear momentum in absence of inertial terms becomes:

$$\sigma_{ji,j} + f_i = 0 \quad [12]$$

where the f_i = -ρ g_i where g_i is the gravitational acceleration vector. The mass of the solid skeleton in a representative elementary volume is:

$$M_s = \int (1-n)\, \rho_s \, dV \quad [13]$$

where $(1-n)\, \rho_s$ represents the volume density of the solid skeleton in the current configuration. See, for example, [9]. The conservation of mass requires that dM_s/dt = 0, so

$$\frac{\partial n}{\partial t} = (1-n)\, \dot{u}_{i,i} \quad [14]$$

The mass conservation equation for pore-water in a representative elementary volume of a freezing soil can be written as

$$\frac{\partial n}{\partial t} + q_{i,i}^{w} + S = 0 \quad [15]$$

In a fully saturated condition $n = \theta_w + \theta_i$ represents the total volumetric water (unfrozen and frozen) content and S is a source term. It should be realized that the porosity value is always smaller than 1 according to its definition ($n = \frac{\theta_v}{\theta_s+\theta_v}$, where θ_v is the total pore volume). Furthermore, the porosity rate function reduces to a small value after an intense growth of ice lenses. Therefore, a porosity threshold, taken as 0.75, is also used in the analysis. However, even though the threshold porosity is reached in some portion of the soil domain, frost heave does not stop since ice continues to grow in other regions (Michalowski et al. 2006). Conservation of energy by considering the phase change becomes

$$C_{app} \frac{\partial T}{\partial t} + q_{i,i}^{T} = 0 \quad [16]$$

where a conduction flux through the volume boundaries, q_i^T, exists. Moreover

$$C_{app} = C_{ph} - \rho_i L_f \frac{\partial \theta_i}{\partial T} \quad [17]$$

is the apparent volumetric heat capacity in which

$$C_{ph} = \rho_w \theta_w C_{pw} + \rho_i \theta_i C_{pi} + \rho_s \theta_s C_{ps} \quad [18]$$

is the volumetric heat capacity of a soil. The C_{pw}, C_{pi} and C_{ps} are the specific heat capacities of water, ice and soil grains, respectively. The value of latent heat L_f is 333kJ/kg.

2.4 Boundary Conditions

Three sets of boundary conditions are enforced relating to the displacement and Cauchy stress vectors; heat flux and temperatures; and water flux and pore pressures. Two sets of vectors must stay continuous at any given traction surface: the Cauchy stress vector, $t_i \overset{\text{def}}{=} \sigma_{ij}\, n_j$ where n_j is a normal unit vector to the surface and the particle displacement vector, u_i . The heat communication boundary conditions, on the other hand, are generally of three types: prescribed temperatures, T, heat flux, $T_{,n_i} \overset{\text{def}}{=} q_0/k_T$, and convective heat exchange, $\alpha(T - T_f)$. Finally, the prescribed pore water pressure, p and water flux $p_{,n} \overset{\text{def}}{=} -q_0^w/k_H$ are applied as the hydraulic boundary conditions. The coupled system of the constitutive, kinematic and conservation equations along with the pertinent boundary conditions are implemented simultaneously in the commercial finite element package COMSOL Multiphysics.

3 MODEL VERIFICATION

The THM model developed in this study are verified by comparing the numerical results with two sets of experimental data found in the literature as well as the temperature field data as explained in this section.

The temperature distribution in the soil sample as well as the amount of frost heave at the surface of the sample are compared with the experimental test performed by Konrad (2005). He performed a freezing experimental test

using a limestone with an initial water content of 21%. The soil column was subjected to a surcharge of 20 kPa. The initial soil column was 97mm. The temperatures of the soil column at the top and bottom were kept at -4.1°C and 1.5°C, respectively. The initial temperature was 3.6°C. The saturated sample was frozen in the axial direction from the top downwards. Water was supplied freely at the warm end. The freezing condition was applied until the steady state condition was reached. During this test, only the temperature profile along the soil sample and the total frost heave at the top of the sample were monitored. The comparison of temperature distribution 20 hours is shown in Figure 1. The frost heave comparison is shown in Figure 2.

Furthermore, the pore-water pressure at the base of the soil column and frost heave at the top of the soil column are verified with the experimental test results provided by Tiedje (2015). The sandy-silt soil was used to conduct the freezing test to examine frost heave. The 0.2 m-height soil column had an initial void ratio of 0.53 (initial porosity of 0.35). The soil sample was initially saturated. The initial soil temperature was 4.5°C. A constant temperature of -3.0°C and 3.2°C was applied to the top and bottom surface, respectively. The applied overburden pressure was 20 kPa. The entire test lasted for 212 hours. The test was conducted without any external water supply. The comparison is given in Figure 3.

In the numerical simulation performed by the THM model developed in this study, the input values are as follows: 1) in the unfrozen water content curve $(\theta_w = \theta_r + (\theta_{wo} - \theta_r)e^{a(T-T_0)}$: $\theta_r = 0.058$, $T_0 = 0°C$ and $a = 0.16\,℃^{-1}$ 2) in the porosity rate function: $\dot{\theta}_m = 6.02 \times 10^{-5}\,s^{-1}$; $T_m = -0.87\,℃^{-1}\}$; $g_T = 100\,℃/\mathrm{m}$ and $\zeta = 0.73\,MPa$; 3) in the poroelastic constitutive model: $\alpha = 0.99975$, the frozen and unfrozen Young's module of the limestone is assumed to be 4,000 kPa and 10,000kPa; for sandy-silt soil, Young's module is assumed to be 1,000 kPa and 5,000 kPa; 3) the hydraulic conductivity of $K_H = 10^{-10}m/s$ is used for of the limestone; for sandy-silt soil, the hydraulic conductivity is defined as a smooth step function in which the unfrozen and frozen hydraulic conductivity is $10^{-7}m/s$ and $10^{-10}m/s$, respectively. The transition temperature interval about the freezing point is defined as 2.5K, as shown in Figure 4 and 4) for the thermal analysis, the typical values for the thermal properties can be seen in Table 1.

Table 1. Soil thermal properties

Material	Density (kg/m^3)	Thermal conductivity $(W/(m \cdot K))$	Heat capacity $J/(kg \cdot K))$
Soil skeleton	2620	1.95	900
Water	1000	0.56	4180
Ice	917	2.24	2000

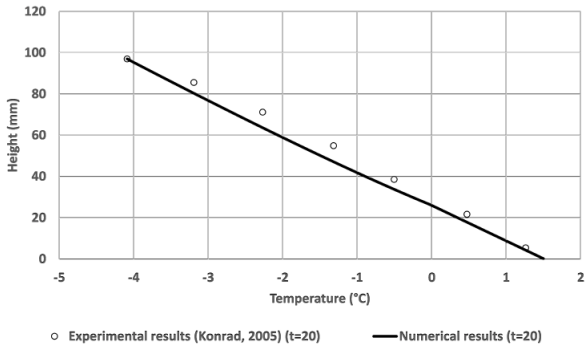

Figure 1. Temperature distribution at 20 hours

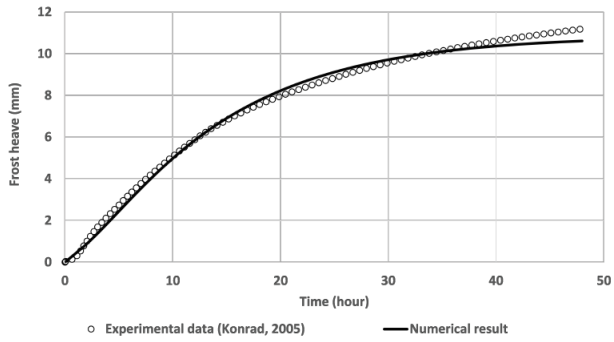

Figure 2. Frost heave during the test (Konrad 2005): experimental data vs numerical results

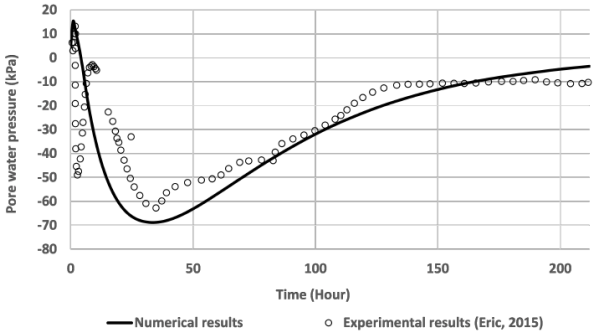

Figure 3 Pore-water pressure distribution at the base during the test (from Tiedje 2015): experimental data vs numerical results

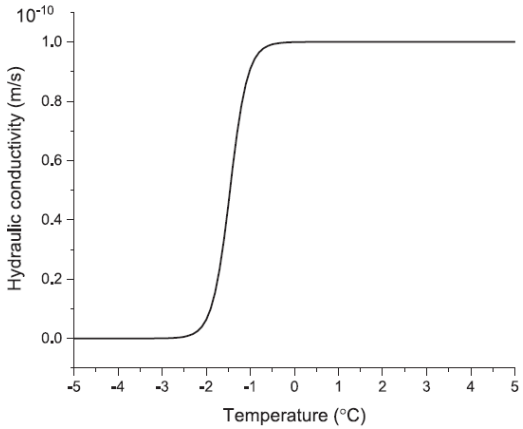

Figure 4 Hydraulic conductivity transition function distribution under various temperature (Liu et al. 2019)

4 THM MODELING OF FROST-SUSCEPTIBLE SOILS IN DOUBLE-BARREL CULVERT SITES: A CASE STUDY

4.1 Field Monitoring Program

The double-barrel culvert sites studied in this paper is part of a comprehensive project consists of five instrumented culvert sites located along the provincial trunk highway 68 (PTH-68), between the Town of Arborg and Lake Winnipeg in Manitoba, Canada. The project aims to study different innovative culvert construction methods including the effect of the transition slope between the natural soil and backfill of the culverts, backfill materials, and the application of geosynthetics to reduce the road roughness and deformation over culverts. For more information about the features of each site, see (Kavanagh et al. 2017) and (Moussa et al. 2018). The site has a pavement structure comprising of 100 mm asphalt layer followed 525 mm and 500 mm granular base. The granular base in both sites is underlain by the culvert backfill resting on high plastic clay subgrade. The culvert at the site is composed of a 2,225 mm clay backfill followed by a 1,250 mm granular. The double-barrel culverts have an outer diameter of 2.1 m. The thickness of the culverts is 15 cm.

The instrumentation program consists of monitoring the ground thermal profile near the culvert's openings by the equally spaced thermistors, which are placed around the culvert barrels in U-shaped and L-shaped strings (Moussa et al. 2018).

4.2 Numerical Modeling

An external forced convection is considered as the boundary conditions at the pavement and culvert surfaces. The convection term, q_{conv}, is temperature- and time-dependent and can be calculated using the following equation:

$$q_{conv}(t) = h_{conv}(T_a(t) - T_s(t)) \quad [19]$$

where T_a (°C) is the ambient air temperature and T_s (°C) is the temperature at the pavement and culverts surfaces. The convection heat transfer coefficient, h_{conv}, depends mainly on conditions on the boundary layer such as wind speed and ambient temperature (Incropera et al. 2007). An adiabatic condition is considered at both vertical sides and the bottom of the domain. The thermal properties used in the numerical analysis for different soil layers and the precast culvert are presented in Table 2.

Table 2. Material thermal properties

Material	Thermal conductivity $(W/(m \cdot K))$	Heat capacity $J/(kg \cdot K))$
Asphalt	1.8	674
Granular base	1.5	1200
Clay backfill	1.1	2000
Granular backfill	1.5	1200
Precast culvert	0.25	1174

The boundary conditions considered in the analysis are summarized in Figure 5. The mechanical properties used in the numerical analysis for different soil layers and the precast culvert can be seen in Table 3. It should be noted that the contour plots presented hereafter only illustrate the field close to the culvert's openings (a total width of 20 m) to highlight their effect.

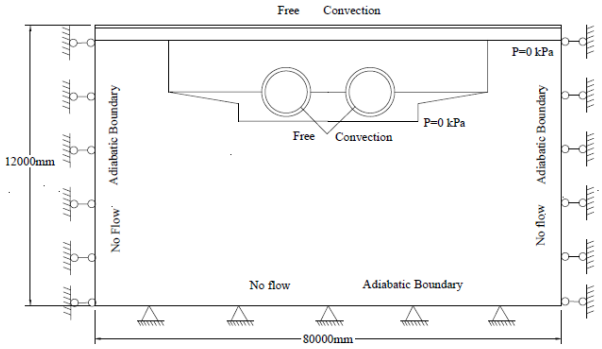

Figure 5. Summary of boundary conditions for the THM analysis

Table 3. Material mechanical properties

Material	Young's Modulus (MPa)	Poisson's ratio (-)	Density (kg/m^3)
Asphalt	2.7×10^6	0.20	2371
Granular base	200	0.30	1700
Clay backfill	100	0.34	1600
Granular backfill	200	0.30	1700
Precast culvert	5×10^6	0.15	3200

The input values in the THM model for the clay subgrade are: 1) in the unfrozen water content curve: θ_r = 0.058, θ_{w0} = 0.29, T_0 = 0°C and a = 0:16°C; 2) in the porosity rate function: $\dot{\theta}_m$= 5.78×10^7 s^{-1}, T_m = -0.87°C, g_T

=100°C/m and ζ = 0.73MPa; 3) in the poroelastic constitutive model: α = 0.99975, the unfrozen and frozen Young's module is assumed to be 5,000 kPa and 10,000kPa; The hydraulic conductivity is defined as smoothed step function in which the unfrozen and frozen hydraulic conductivity is 10^{-8} m/s and 10^{-12} m/s, respectively. The transitional zone is defined as 2K.

4.3 Results and Discussions

Initially, the temperature in the clay subgrade is above the freezing point everywhere in the domain. The initial temperature distribution is given in Figure 6. The field measurement and numerical results are compared in Figure 7. Due to the heat convection at the surface of pavement and culverts openings, the temperature of the soil located just below the culverts starts to decrease below the freezing point. As shown in Figure 8, this freezing effect is accompanied with the frost heave lifting the culverts.

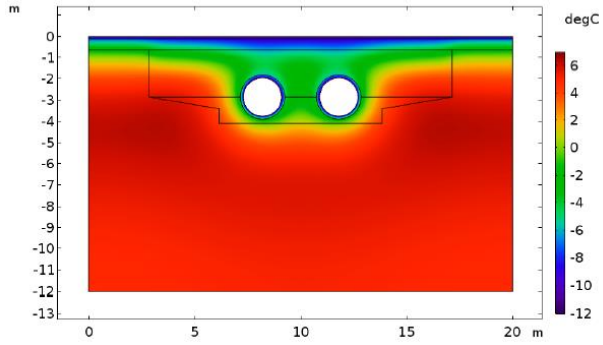

Figure 6 Initial temperature distribution at the side

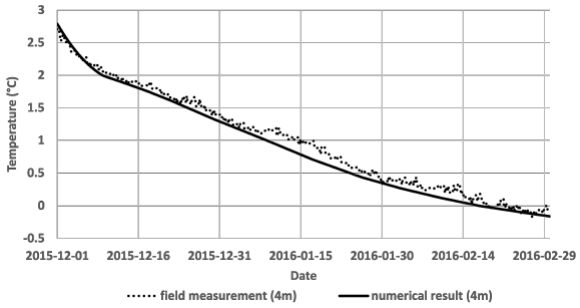

Figure 7 Temperature distribution at a depth of 4 m (solid line denotes data from simulation and dot line denotes data from field measurement)

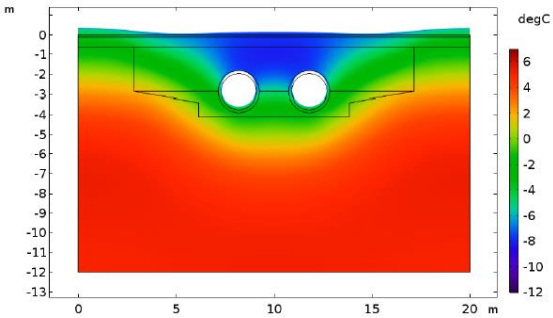

Figure 8 Deformation and temperature distribution after 90 days

The cumulative displacement along the road surface, after 90 days from the start of the freezing period, is illustrated in Figure 9. It is shown that frost heave, at the pavement surface, at a distance of 10 m away from the centerline and at the mid-distance between the culvert structures are 31 mm and 12 mm, respectively after 90 days. This conclusion is in accordance with field observations that culverts seem to settle during the freezing period.

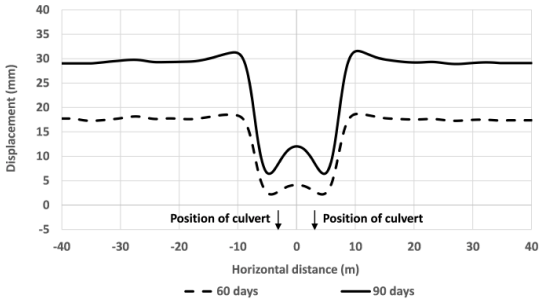

Figure 9 Frost heave along the pavement surface after 60 and 90 days

The distribution of pore-water pressure in soil is important in terms of the soil strength and the bearing capacity of the pavement foundation. The freezing of pore-water generates negative pore-water pressure or suction.

It can be seen from Figure 10 that suction is quickly built up in the side soils due to the faster heat loss. The maximum suction is estimated to be -40 kPa and -80 kPa after 60 days and 90 days, respectively.

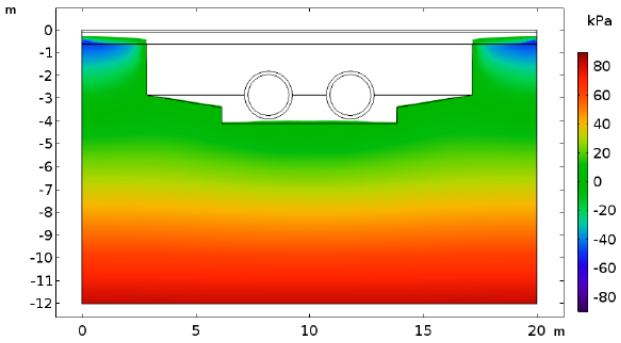

Figure 10 Porewater pressure distribution after 90 days

5 EFFECT OF INSULATION ON FROST HEAVE IN DOUBLE-BARREL CULVERT SITES

The differential displacement is detrimental to the structural integrity of culverts and pavement. The differential displacement occurs mainly due to the different frost heave rate for natural soils at the sides of culverts and soils beneath the culverts. Since overburden pressure is predetermined by the structure design, controlling the temperature distribution becomes the key to minimize the frost heave and differential displacement.

Insulating materials can be used to minimize the heat exchange between the cooling sources (such as pavement surface and culvert openings) and surrounding soils so that the soil temperature can be maintained above the freezing

point. In these conditions, frost heave can be largely decreased or even avoided.

To the best of the authors' knowledge, the effect of the distribution of thermal insulation and its geometry on differential frost action and frost heave of double-barrel culvert is poorly documented. In a recent study (Moussa et al. 2018), a parametric study is carried out to determine the most effective position of insulation near culvert to minimize the frost depth in double-barrel culvert sites.

This section aims to study the effect of insulation location with respect to culverts openings on frost heave and differential displacement at the pavement surface. Three different insulation configurations are studied. Method A) a circular insulation on the outer surface of the culverts; Method B) a horizontal insulation at the top of the clay subgrade below the culverts; and Method C) a horizontal insulation at the top of the frost-susceptible subgrade below the culverts and at the sides of the culvert structure. The culverts layout with different insulation methods can be seen in Figure 11. The first two configurations have been found to be the most effective in terms of thermal performance according to (Moussa et al. 2018).

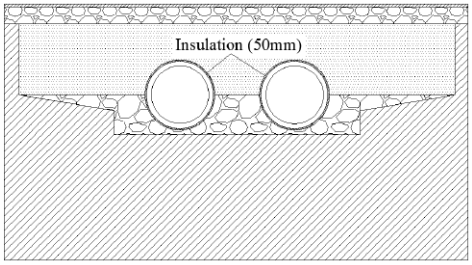

(a) insulation method A

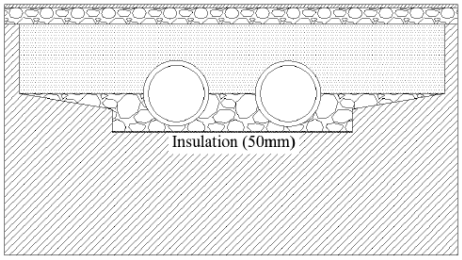

(b) insulation method B

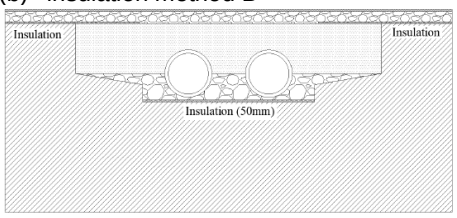

(c) insulation method C

Figure 11 Summary of insulation methods studied in this paper (a) method A (b) method B (c) method C

The deformation and temperature distribution in the domain by using a circular insulation on the outer surface of the culverts, after 90 days from the start of the freezing period, are illustrated in Figure 12.

To give a better insight into the structural integrity and roughness of the road, the differential deformation due to frost heave at the pavement surface is shown in Figure 12. It is shown that the circular insulation on the outer surface of the culverts reduces effectively the heat exchange between the culvert's openings and the surrounding soils. In this case, the frost heave can be avoided in frost-susceptible soils below the culverts. However, with the advance of frost penetration, the frost heave at the side soils develops gradually. On the other hand, the circular insulation on the outer surface of the culverts does not have any impact on the frost heave of the side soils. Consequently, by preventing frost heave in frost-susceptible soils below the culverts by using an insulation on the outer surface of the culverts, the differential displacement at the pavement surface becomes more significant.

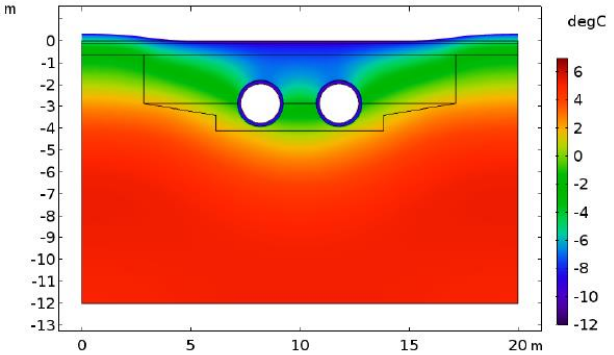

Figure 12 Deformation and temperature distribution after 90 days using insulation method A

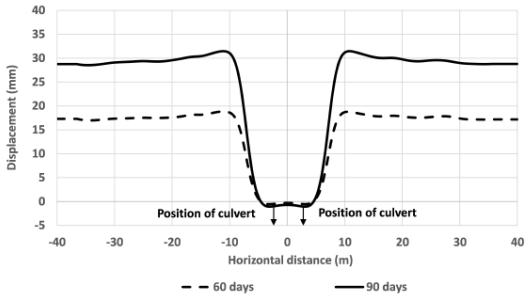

Figure 13 Deformation along the pavement surface after 60 days and 90 days using insulation method A

It is shown that although the temperature distribution in the ground using insulation methods A and B are different, the overall frost heave and differential displacement are similar. Both methods A and B can largely reduce the frost heave in the clay subgrades below the culverts. However, the differential displacement using both methods is increased. On the other hand, the insulation methods A and B cannot efficiently remove differential deformations at the pavement surface.

To effectively remove the differential deformation at the pavement surface, a horizontal insulation is placed at the top of the natural frost-susceptible subgrade below the culverts and at both sides of the double-barrel culvert structure. An insulation thickness of 50 mm and 100 mm for the sides are studied in this section. The deformation

and temperature distribution using insulation method C (100 mm) are illustrated in Figure 14. The displacements after 90 days along the pavement surface by using the insulation methods B and C are compared in Figure 15.

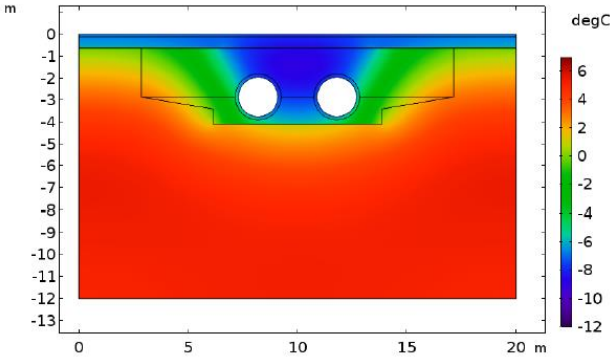

Figure 14 Deformation and temperature distribution in the domain by using the insulation method C

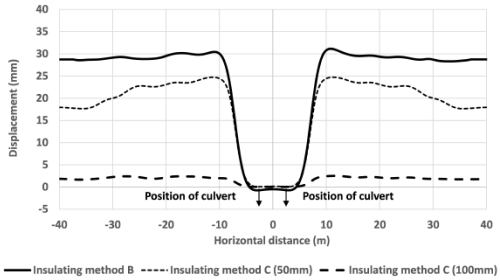

Figure 15 Deformation along the pavement surface by using the insulation methods B and C after 90 days

It is shown that differential displacement can be more than 25 mm by using 50 mm thickness insulation at the sides. It is concluded that placing insulation at the top of the frost-susceptible soil is necessary to mitigate the differential deformation along the pavement surface. By applying the insulation method C with 100 mm thickness insulation at sides, the differential displacement and the maximum frost heave are reduced to 2.4 mm, as shown in Figure 15. Therefore, the insulation method C is recommended.

6 CONCLUSION

In this paper, a fully coupled thermal-hydro-mechanical model is presented by using the theory of poroelasticity and a porosity rate function to numerically study the phenomena of frost heave in double-barrel culvert sites. It is concluded that the THM model proposed in this study is able to accurately predict frost heave, temperature and pore-water pressure distribution in the ground. The numerical results showed a good agreement with the experimental test data and field measurement. Furthermore, for double-barrel culverts, using an insulation at the top of the frost-susceptible subgrade below the culverts and at the sides of the culvert structure (insulation method C with 100 mm insulation thickness at sides) can be applied to effectively decrease the frost heave and the corresponding differential displacement at the pavement surface.

7 ACKNOWLEDGMENT

This research was partially supported by University Research Grants Program (2018) and Strat-Up Fund (2015-2018), University of Manitoba. The authors would like to acknowledge the software platform provided by COMSOL Inc. and CMC Microsystems.

8 REFERENCES

Konrad, Jean-Marie. 2005. *Estimation of the Segregation Potential of Fine-Grained Soils Using the Frost Heave Response of Two Reference Soils*, Canadian Geotechnical Journal 42(1): 38–50.

Liu, Hongwei, Pooneh Maghoul, and Ahmed Shalaby. 2019. *Optimum Insulation Design for Buried Utilities Subject to Frost Action in Cold Regions Using the Nelder-Mead Algorithm*, International Journal of Heat and Mass Transfer 130: 613–39.

Liu, Hongwei, Pooneh Maghoul, Ahmed Shalaby, and Ako Bahari. 2019. *Thermo-Hydro-Mechanical Modeling of Frost Heave Using the Theory of Poroelasticity for Frost-Susceptible Soils in Double-Barrel Culvert Sites*, Transportation Geotechnics: 100251.

Michalowski, R. L. 1993. *A constitutive model of saturated soils for frost heave simulations*, Cold regions science and technology, 22(1), 47-63.

Michalowski, Radoslaw L., and Ming Zhu. 2006. *Frost Heave Modelling Using Porosity Rate Function*, International Journal for Numerical and Analytical Methods in Geomechanics 30(8): 703–22.

Zhang, Yao, and Radoslaw L. Michalowski. 2015. *Thermal-Hydro-Mechanical Analysis of Frost Heave and Thaw Settlement*. Journal of Geotechnical and Geoenvironmental Engineering 141(7): 04015027.

A Moussa, A Shalaby, L Kavanagh, and P Maghoul. *Use of rigid geofoam insulation to mitigate frost heave at shallow culvert installations*. Journal of Cold Regions Engineering, 33(3), 05019003.

Incropera, Frank P., Adrienne S. Lavine, Theodore L. Bergman, and David P. DeWitt. 2007. *Fundamentals of heat and mass transfer*. Wiley.

Kavanagh, Leonnie, Ahmed Shalaby, Ahmed Moussa, and Scott Sparrow. 2017. *Analysis of Measured Strains in Geotextile-Reinforced Clay Backfill over Through-Grade Culverts in Cold Climates*. No. 17-06559.

Eric Tiedje. 2015. *The Experimental Characterization and Numerical Modelling of Frost Heave*. PhD thesis, McMaster University.